Journal of Medicinal Chemistry

Article

pubs.acs.org/jmc

Design and Nuclear Magnetic Resonance (NMR) Structure Determination of the Second Extracellular Immunoglobulin Tyrosine Kinase A (TrkAIg2) Domain Construct for Binding Site Elucidation in Drug Discovery

Debbie K. Shoemark,[†,⊥] Christopher Williams,[‡,⊥] Mark S. Fahey,[†] Judy J. Watson,[†] Sue J. Tyler,[†] Simon J. Scoltock,[†] Rosamund Z. Ellis,[‡] Elaine Wickenden,[‡] Antony J. Burton,[‡] Jennifer L. Hemmings,[‡] Christopher D. Bailey,[‡] David Dawbarn,[#] David E. Jane,[§] Christine L. Willis,[‡] Richard B. Sessions,[∥] Shelley J. Allen,*[,†] and Matthew P. Crump*[,‡]

[†]School of Clinical Sciences, Level 2, Learning and Research, Southmead Hospital, Bristol BS10 5NB, United Kingdom

[‡]School of Chemistry, University of Bristol, Cantock's Close, Bristol BS8 1TS, United Kingdom

[§]School of Physiology & Pharmacology, University of Bristol, Medical Sciences Building, University Walk, Bristol BS8 1TD, United Kingdom

[∥]School of Biochemistry, University of Bristol, Medical Sciences Building, University Walk, Bristol BS8 1TD, United Kingdom

Supporting Information

ABSTRACT: The tyrosine kinase A (TrkA) receptor is a validated therapeutic intervention point for a wide range of conditions. TrkA activation by nerve growth factor (NGF) binding the second extracellular immunoglobulin (TrkAIg2) domain triggers intracellular signaling cascades. In the periphery, this promotes the pain phenotype and, in the brain, cell survival or differentiation. Reproducible structural information and detailed validation of protein−ligand interactions aid drug discovery. However, the isolated TrkAIg2 domain crystallizes as a β-strand-swapped dimer in the absence of NGF, occluding the binding surface. Here we report the design and structural validation by nuclear magnetic resonance spectroscopy of the first stable, biologically active construct of the TrkAIg2 domain for binding site confirmation. Our structure closely mimics the wild-type fold of TrkAIg2 in complex with NGF (1WWW.pdb), and the $^{1}H-^{15}N$ correlation spectra confirm that both NGF and a competing small molecule interact at the known binding interface in solution.

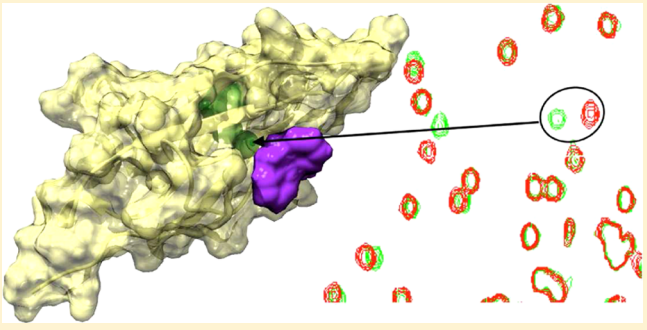

INTRODUCTION

The human tyrosine kinase receptor family is comprised of TrkA, TrkB, and TrkC. TrkA and TrkB have become targets for drug discovery for treating conditions ranging from pain and cancer to schizophrenia and Alzheimer's disease.[1,2] Here we focus on the design and structure determination of a stable construct of the extracellular TrkAIg2 domain suitable for use in NMR to provide binding site information in drug discovery projects.

In the periphery, TrkA mediates nociceptive sensitization when its cognate ligand NGF binds. The Trk receptors are comprised of a leucine/cysteine rich domain and two immunoglobulin-like domains, Ig1 and Ig2, in the extracellular region linked to an intracellular kinase domain by a single membrane-spanning helix. The Ig2 domain is proximal to the cell membrane and provides the NGF binding site as was first indicated by Urfer et al.[3] and later shown by X-ray crystallography.[4,5] NGF is a homodimeric protein presenting two TrkA binding sites on opposite faces of the dimer. The binding of NGF brings together two TrkA receptors triggering autophosphorylation of their intracellular kinase domains. Autophosphorylation provides binding sites for proteins involved in downstream signaling in the phosphatidylinositol-3 (PI3) -kinase, mitogen-activated kinase/extracellular-signal-regulated kinase (MAP kinase/ERK), and phospholipase C-γ (PLC-γ) pathways.[6,7] Consequentially, NGF activation of TrkA modulates the activity of both ligand and voltage-gated ion channels involved in nociception via the following mechanisms. Under resting conditions, the ligand-gated transient receptor potential cation channel vanilloid subfamily member 1 (TRPV1) is constitutively inhibited by phosphoinositol 4,5-bisphosphate (PIP2) on nociceptors. The activation of PLC-γ downstream of TrkA activation by NGF relieves this constitutive inhibition by hydrolyzing PIP2 to inositol 1,4,5-trisphosphate (IP3) and

Received: August 27, 2014
Published: December 2, 2014

   dx.doi.org/10.1021/jm501307e | J. Med. Chem. 2015, 58, 767−777

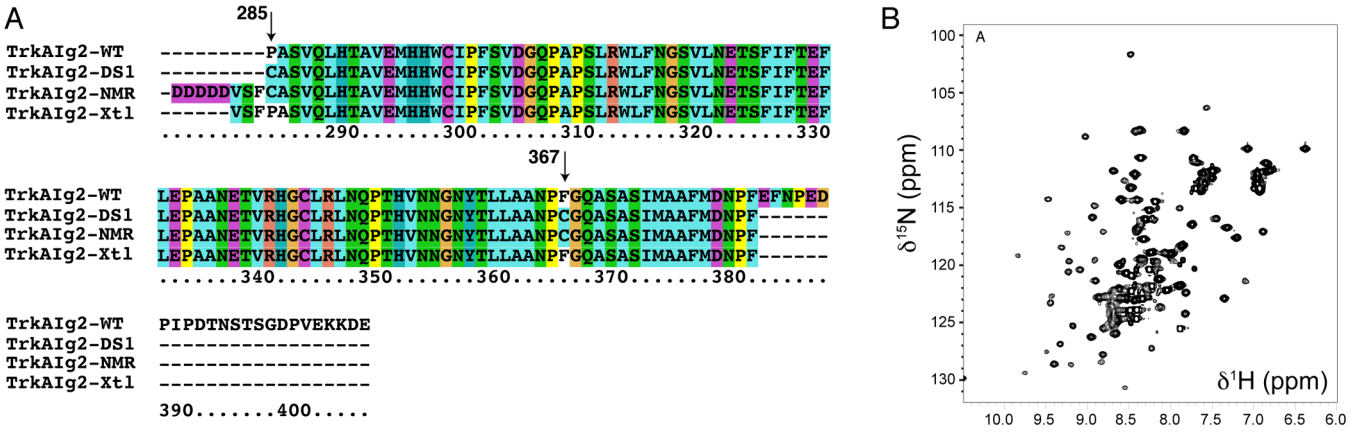

Figure 1. (A) Sequence comparison of "wild-type" TrkAIg2-WT domain, the first-generation engineered cysteine mutant (TrkAIg2-DS1), the final construct produced for solution NMR studies (TrkAIg2-NMR), and the construct used in X-ray crystallographic studies of the strand-swapped dimer (TrkAIg2-Xt1).[20] (B) $^{1}H-^{15}N$ HSQC spectra of the wild-type construct TrkAIg2-WT. The amide peak dispersal indicates that the protein is not a homogeneous population or that some of the structure is disordered.

diacylglycerol.[6] This lowers the threshold of activation of TRPV1 and other ion channels. Pain signaling is enhanced by the release of brain derived neurotrophic factor (BDNF), substance P, and other peptides which are transported to the dorsal root ganglion (DRG), subsequently promoting central pain perception.[8] The activation of TrkA by NGF thus initiates the chronic pain phenotype by increasing nociceptor sensitivity to further stimulus.[9] During the sensitization process, TrkA expression is itself up-regulated on nociceptors, as are the ion channels Nav1.8, P2XY, and TRPV1.[10]

However, within the brain, TrkA function is fundamental to memory formation and learning.[1] Cholinergic cells of the basal forebrain extend axons into the hippocampus and cerebral cortex and depend on the supply of NGF delivered by axonal retrograde transport.[11] Activation of TrkA by NGF triggers the aforementioned signaling cascades to provide support for neurite growth and repair and maintenance of effective connectivity between the cholinergic basal forebrain, hippocampus, and the cortex for the formation of new memories. Early in the progression of Alzheimer's disease, TrkA/NGF signaling in the cholinergic cells of the basal forebrain is compromised, the cells undergo axonal withdrawal, and as a result, brain regions no longer communicate efficiently. This contributes to short-term memory impairment and confusion.

TrkA is a validated target for pain therapeutics in both animal models and in the clinic. NGF based therapeutics in animal models of pain including the NGF binding domain on TrkA (TrkAIg2)[12−15] and anti-NGF antibodies including Tanezumab[16,17] have successfully provided relief from acute and chronic pain states in clinical trials.[18] However, several antibody therapies have had serious side effects[19] which may arise from the high affinity of the antibody/target interaction combined with the very long half-life of the NGF antibody, making bioavailability hard to predict and hence control by dosing.

Identifying small molecule therapeutics targeted to the extracellular TrkA domain to disrupt the TrkA/NGF protein−protein interaction provides a major challenge, and high-throughput screens have failed to produce small molecule antagonists to this target. Kinase inhibitors specific for TrkA are difficult to achieve as the intracellular kinase domains are highly conserved between the Trk receptors: A to B, 75% identity, A to C, 76% identity, and B to C, 82% identity and all have almost identical ATP binding sites.

Targeting the extracellular NGF binding domain of TrkA, the TrkAIg2 domain, provides potential advantages for two main reasons: influencing the extracellular ligand binding interaction represents the preamplification stage in the signaling cascades where nature "fine-tunes" receptor-mediated events; the neurotrophin binding domains share lower sequence identity between Trk receptors: A to B, 46%, A to C, 41%, and B to C, 47%, making specific targeting more readily achievable. Compounds that can prevent NGF-mediated activation of TrkA on peripheral nociceptors will be useful in the management of pain and those capable of acting centrally to augment NGF-mediated activation of TrkA could be developed as Alzheimer's therapeutics to support the cholinergic system.

To develop TrkAIg2 domain binders, access to reproducible structural information is required to confirm the compound binding site. Crystallography has proven to be problematic because at high concentrations the isolated Ig2 domain forms β-strand-swapped dimers (1WWA.pdb) in the absence of its cognate ligand NGF and is thus biologically inactive.[4] Strand-swapping occludes not only the NGF binding site but also the compound binding sites targeted.

We describe the design and validation of a TrkAIg2-NMR construct in which we have stabilized the native fold (not strand-swapped) and retained biological activity. Here we use solution NMR to determine the three-dimensional structure of the protein and validate the use of the construct using NGF and a small molecule (amitriptyline) in both NMR binding experiments and functional assays. This approach should greatly facilitate the development of small molecule leads for modulating the activity of TrkA and related receptors.

RESULTS AND DISCUSSION

Design of the NMR Construct TrkAIg2-NMR. Initially, we selected an in-house construct spanning the second Ig domain of TrkA that we refer to as "wild-type" TrkAIg2 (TrkAIg2-WT) (Figure 1A). This construct has been used successfully to sequester NGF and abrogate pain in a number of in vivo models[12−15] and was therefore used for initial NMR studies. A ^{15}N-labeled sample of the TrkAIg2-WT construct was prepared and a two-dimensional $^{1}H-^{15}N$ HSQC NMR spectrum recorded (Figure 1B). This spectrum displayed many unfavorable features for structural and ligand-binding assays, including overlap and

dx.doi.org/10.1021/jm501307e | J. Med. Chem. 2015, 58, 767−777

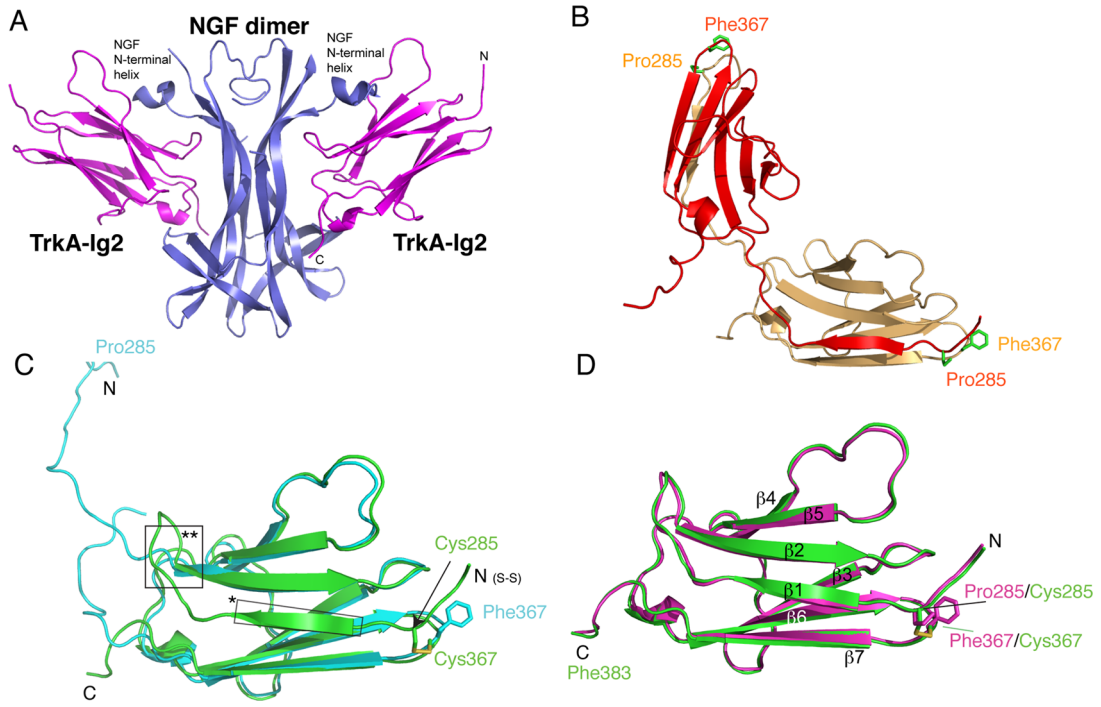

Figure 2. Comparison of X-ray crystallographic structures and modeled TrkA-Ig2 in free forms and complexed with NGF. (A) Crystal structure of the complex between NGF and TrkA-Ig2 (1WWW.pdb)[20] with two molecules of TrkA-Ig2 shown in magenta in binding to an NGF dimer (slate). (B) Crystal structure of two molecules of TrkA-Ig2 (red and light-orange) in the absence of NGF forming a strand-swapped dimer (1WWA.pdb).[4] (C) Superposition of the X-ray structure of a further strand-swapped dimer of TrkAIg2 (PDB code 1HE7)[20] (cyan) with the position of P285 and F367 highlighted. The structure of modeled domain 5 (green) is shown incorporating the P285C and F367C mutations and the new disulfide bond after energy minimization. The fold is predicted to be minimally perturbed when this disulfide is introduced. The N-terminal strand in the modeled construct is highlighted with *, and the point at which the non- and strand-swapped dimers diverge is indicated by **. (D) Similarly, superposition of the minimized disulfide bridged construct shows close structural similarity with the packing of the N-terminal β-strand in the NGF bound crystal structure (1WWW.pdb).

heterogeneity of signal intensity (e.g., a mixture of intense and weak broadened cross-peaks).

To engineer a construct for use in the absence of NGF, we re-examined known crystal structures of these proteins. The X-ray crystallographic study of the wild-type single TrkA-Ig2 domain (Figure 2A) bound to NGF previously revealed two molecules of the TrkA-Ig2 domain bound to a central NGF dimer.[5] An extensive interface was observed between NGF and the individual TrkA-Ig2 domains, but there were no direct contacts between the TrkA-Ig2 domains themselves. When studied in isolation, however, the Ig2 domains from TrkA, TrkB, and TrkC have all been shown to form strand-swapped dimers in solved crystal structures (Figure 2B), an association that occludes the interaction site on TrkA for NGF. Therefore, at high concentrations, the formation of oligomeric[4] species in addition to unstructured regions might explain the poor NMR characteristics of the TrkAIg2-WT construct. Figure 2C shows an overlay of a single TrkA-Ig2 domain chain from the strand-swapped crystal structure 1HE7.pdb with a single chain from the crystal structure 1WWW.pdb in complex with NGF. The strand-swapped structure of TrkA-Ig2 (residues 285−413), studied by Robertson et al., revealed a stable core structure extending to P382 after which no electron density was observed.[20] The C-terminal was presumed to be flexible and might not therefore be ideal for solution-state NMR studies. Therefore, the C-terminal was truncated to end in the residues DNPF (383) (Figure 1A). To prevent β-strands swapping between adjacent monomers at high concentrations, an additional disulfide bond was also introduced to act as an intramolecular staple between β-strand 1 (P285C) and the β-hairpin between strands 6 and 7 (F367C, Figure 1A) to yield our first-generation construct TrkAIg2-DS1. The disulfide bridge was modeled onto chain X of TrkA from the crystal structure 1WWW.pdb and then energy minimized using Discover 2.98 (Accelrys) (Figure 2D). These residues were chosen because they were suitably distant from the NGF binding face of the protein and therefore less likely to influence the binding of compounds to the target site. P285 and F367 were already almost the optimal distance apart required for disulfide bond formation. In the crystal structure, their side chains were oriented toward each other so that disulfide formation between two cysteines at these positions would be predicted to cause minimal distortion to the overall fold. Importantly, these residues fulfilled another necessary criterion[21] predicted to produce a hyper-stable native state, namely they were not involved in the hydrogen bonding pattern of the β-sheet.

Comparison of the predicted model of TrkAIg2-DS1 with the crystal structure of the strand-swapped dimer (Figure 2C) shows the expected drastic change in the packing of the N-terminal strand but minimal perturbation to the remainder of the protein. Similarly, comparison of the predicted model with the non-strand-swapped crystal structure of the TrkA-Ig2 domain in complex with NGF shows only small perturbations in the region of the disulfide bridge which were unlikely to influence the more distant NGF binding site (Figure 2D).

TrkAIg2-DS1 was expressed and purified but yields of protein were low, so a further construct which included an additional 5 N-terminal aspartates (TrkAIg2-NMR) was produced (Figure 1A). The hypothesis was that an increased overall negative

dx.doi.org/10.1021/jm501307e | J. Med. Chem. 2015, 58, 767−777

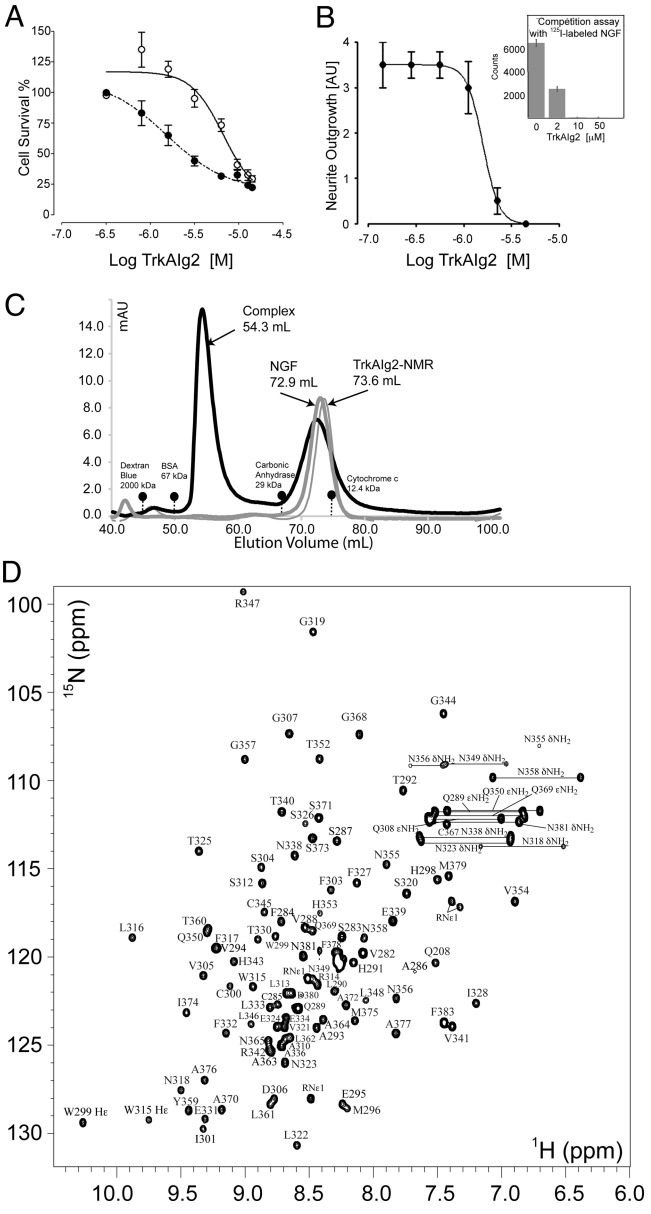

Figure 3. Functional and biophysical characterization of TrkAIg2-NMR compared to TrkAIg2-WT. (A) TrkAIg2-NMR and TrkAIg2-WT effect on NGF-dependent cell proliferation in PC12 cells. Both the TrkAIg2-WT (closed circles, EC_{50} 0.48 μM) and the TrkAIg2-NMR (open circles, EC_{50} 2.1 μM) forms were able to sequester NGF and prevent cell proliferation in a dose-dependent manner. (B) The effect of TrkAIg2-NMR on NGF-mediated neurite outgrowth in PC12 cells: 0.04 nM NGF was added to PC12 cells in addition to a range of concentrations of ^{15}N labeled TrkAIg2. The TrkAIg2-NMR construct inhibited neurite outgrowth with an EC_{50} 1.59 μM. Inset: ^{15}N-labeled TrkAIg2-NMR mediated sequestration of ^{125}I-labeled NGF in a competition assay against full-length human TrkA receptors expressed on HEK cells, with an approximate IC_{50} of 2 μM. (C) Complex formation between TrkAIg2-NMR and NGF. TrkAIg2-NMR and mouse NGF were applied to a gel filtration S75 column, separately and as a 1:1 ratio complex of two monomers of TrkAIg2-NMR with one dimer of NGF. The TrkAIg2-NMR/NGF complex (Mwt 51 kDa) was shown to run at 57 kDa as estimated by a calibration curve. Alone, TrkAIg2-NMR (Mwt of monomer is 11.9 kDa) ran at 17 kDa; NGF (27 kDa dimer) ran at 18.8 kDa. (D) ^{1}H–^{15}N HSQC spectra of TrkAIg2-NMR, showing vastly improved homogeneity of peak intensity and line shape.

charge (p*I* with aspartates 4.52) might reduce nonspecific association during refolding and reduce the potential for inappropriate disulfide bonding during the refold by not having the cysteine at position one in the sequence.

Yields of the second-generation protein, termed TrkAIg2-NMR, were improved as the proportion of protein aggregating on refold was significantly reduced. Biological activity was determined through the ability of TrkA constructs to bind and sequester NGF. The TrkAIg2-NMR reduced cell survival (Figure 3A) with an EC_{50} of 2.1 μM compared with TrkAIg2-WT EC_{50} 0.48 μM). TrkAIg2-NMR inhibition of NGF-induced neurite outgrowth on PC12 cells (Figure 3B) gave an EC_{50} of 1.59 μM. This construct also sequestered radiolabeled NGF in competition assays with an approximate IC_{50} of 5 μM on HEK cells expressing human TrkA (Figure 3B, inset). Biological activity was confirmed for each batch of TrkAIg2-NMR protein produced. A MALDI-TOF spectrum confirmed the presence of a single monomeric species and no disulfide-linked dimer was detected and native gel electrophoresis showed a single band (Supporting Information, Figure S1). Analytical ultracentrifugation of the TrkAIg2-NMR construct confirmed that the protein was monomeric under the conditions used for the NMR studies (Supporting Information, Figure S1), and gel filtration showed a single symmetrical peak (Figure 3C). Taken together, these results indicate the construct was a monomeric homogeneous fold.

A ^{1}H–^{15}N HSQC was recorded on a ^{15}N-labeled sample of TrkAIg2-NMR (Figure 3D) and showed distinct improvements to both peak dispersion and uniformity of peak height. This construct also had the advantage of being stable for at least three months at 25 °C and provided reproducible HSQC spectra between preparations.

Assignment and Three-Dimensional Structure Determination. The assignment of the ^{1}H, ^{13}C, and ^{15}N resonances of TrkAIg2 were obtained using a ^{13}C, ^{15}N labeled sample of TrkAIg2-NMR and triple resonance experiments recorded at 600 MHz. Overall, 98% of the backbone resonances could be assigned, with missing residues being located in the N-terminal Asp-rich region; 94% of the side-chain resonances could be assigned. Again missing resonances were primarily located in the N-terminal region.

The solution structure was determined using a total of 182 dihedral angles, 46 hydrogen bonds, and 2053 NOEs derived from 3D ^{15}N-edited NOESY-HSQC, ^{13}C aromatic HSQC-NOESY, and simultaneous ^{15}N/^{13}C-edited NOESY spectra. The final twenty structures chosen to represent the ensemble of NMR structures (Figure 4A) were consistent with both experimental data and standard covalent geometry, displaying no violations greater than 0.5 Å for distance restraints or 5° for dihedral angles. The averaged structure for the ensemble highlights the position of the disulfide staple (Figure 4B). Details of the final set of structural restraints and their violations within the final ensemble are listed in Table 1.

The core of TrkAIg2-NMR is well-defined, with a backbone rmsd from the mean over the regular secondary structure elements of 0.38 Å for the ensemble of structures. As expected, the solution structure forms an Ig-like fold consisting of a β-sandwich formed by two β-sheets. The structure is highly similar to the 2.2 Å crystal structure of TrkA in complex with NGF solved at pH 5.0 (1WWW.pdb)[5] with a backbone rmsd over the secondary structure elements of 0.68 Å (ProFit v2.5) (Figure 4C). As expected, the introduction of a disulfide bond between

dx.doi.org/10.1021/jm501307e | J. Med. Chem. 2015, 58, 767–777

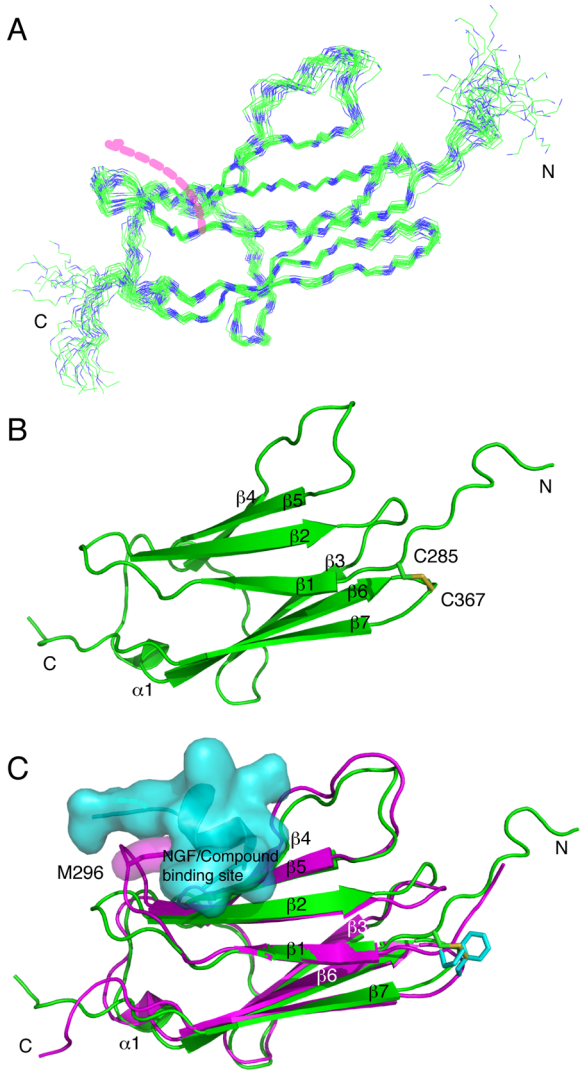

Figure 4. Solution structure of TrkAIg2-NMR and comparison with the crystal structure. (A) The ensemble of 20 TrkAIg2-NMR domain structures. The NGF binding groove is indicated with a dotted line. (B) The closest to the geometric average solution structure with the position of the disulfide staple shown between C285 and C367. (C) An overlay of chain X from the crystal structure of the TrkAIg2/NGF complex (magenta, 1WWW.pdb)[20] and the closest to the geometric average NMR model of the TrkAIg2-NMR (green) construct showing that the disulfide bridge has not disrupted the global protein fold.

Table 1. Structural Restraints and Violations of the Final Structures

completeness of resonance assignments[a]	
backbone/non-H (%)	92.8/93.6
side chain H/non-H (%)	94.7/75.7
conformational restricting restraints	
total NOE restraints	2053
intraresidue	910
sequential/medium range (residue i to i+(1−5)	637
long-range	453
ambiguous	53
dihedral angle restraints	182
hydrogen-bonds restraints	46
disulfide restraints	2
residual restraint violations[b]	
average no. of distance angle violations per structure	
>0.1 (Å)	3.88
>0.3 (Å)	0
>0.5(Å)	0
average no. of dihedral angle violations per structure	
>5°	0
model quality[b]	
rmsd backbone 2° structure atoms (Å)	0.38 (±0.068)
rmsd heavy 2° structure atoms (Å)	0.77 (±0.066)
rmsd backbone all atoms (Å)	1.34 (±0.30)
rmsd heavy all atoms (Å)	1.81 (±0.32)
rmsd bond lengths (Å)	0.016
rmsd bond angles (deg)	1.3
MolProbity Ramachandran statistics[c]	
most favored regions (%)	97.3
allowed regions (%)	2.4
disallowed regions (%)	0.2
global quality scores (raw/Z scores)[c]	
Verfiy3D	0.27/−3.05
ProsaII	0.23/−1.74
Procheck (Φ−ψ)	−0.58/−1.97
Procheck (all)	−0.45/−2.66
MolProbity clash score	15.97/−1.12
BMRB accession number	19824
PDB ID code	4crp

[a]CcpNmr Analysis v2.3.1.[28,29] [b]CNS/Aria 2.3.[32−34] [c]Calculated using PSVS 1.5.[35]

P285 and F367 to help stabilize the protein does not affect the overall structure.

Minor differences in the solution and crystal structures are observed in the loop regions due to pH or conformational changes. The complex was crystallized by hanging drop in 1:1 protein solution:Hampton screen. The protein solution was 10 mg mL^{-1} complex (TrkA and NGF) in 0.1 M NaCl, 0.1 M bicine, pH 8.5, the Hampton screen condition comprised of 24% PEG 3350, 0.1 M citric acid, pH 5.0 (1WWW.pdb). Buffer conditions for the NMR were 100 mM sodium phosphate pH 6.9 and 10 mM NaCl. No evidence of dimer formation was observed in the NMR experiments, and testing the calculated models against a possible dimeric stoichiometry gave no improvement in the fit to the NOE data or minimized energies.

Structure−Function Validation: The TrkAIg2-NMR Protein Binds NGF, the Cognate Ligand for TrkA. We then tested whether we could detect a direct protein−protein interaction in solution under conditions used for NMR with the TrkA receptor's cognate ligand, the cytokine NGF (from mouse submaxillary salivary glands[22]). NGF readily adsorbs onto many surfaces,[23] but reversible acid denaturation reduces this propensity. NGF is therefore stored in sodium acetate at pH 2 to minimize losses. A single-shot NMR assay was recorded to ensure that no pH perturbation occurred when the complex was formed as 650 μg of NGF (preadjusted to pH 6.9) was added to a solution of ^{15}N-TrkAIg2-NMR to approach a 1:1 stoichiometry. Complex formation was confirmed by gel filtration (Figure 3C). Figure 5A shows the ^{1}H−^{15}N HSQC spectra before (black) and after (red) the addition of a stoichiometric concentration of NGF. A number of residues show either amide chemical shift perturbations (CSPs) or are significantly line broadened in the presence of NGF (Figure 5B). These perturbed residues were mapped onto the crystal structure of the TrkAIg2 domain bound to NGF and are shown in Figure 5C,D. Although the CSPs are <0.15 ppm,[24] the predominant spectral changes cluster around

dx.doi.org/10.1021/jm501307e | J. Med. Chem. 2015, 58, 767−777

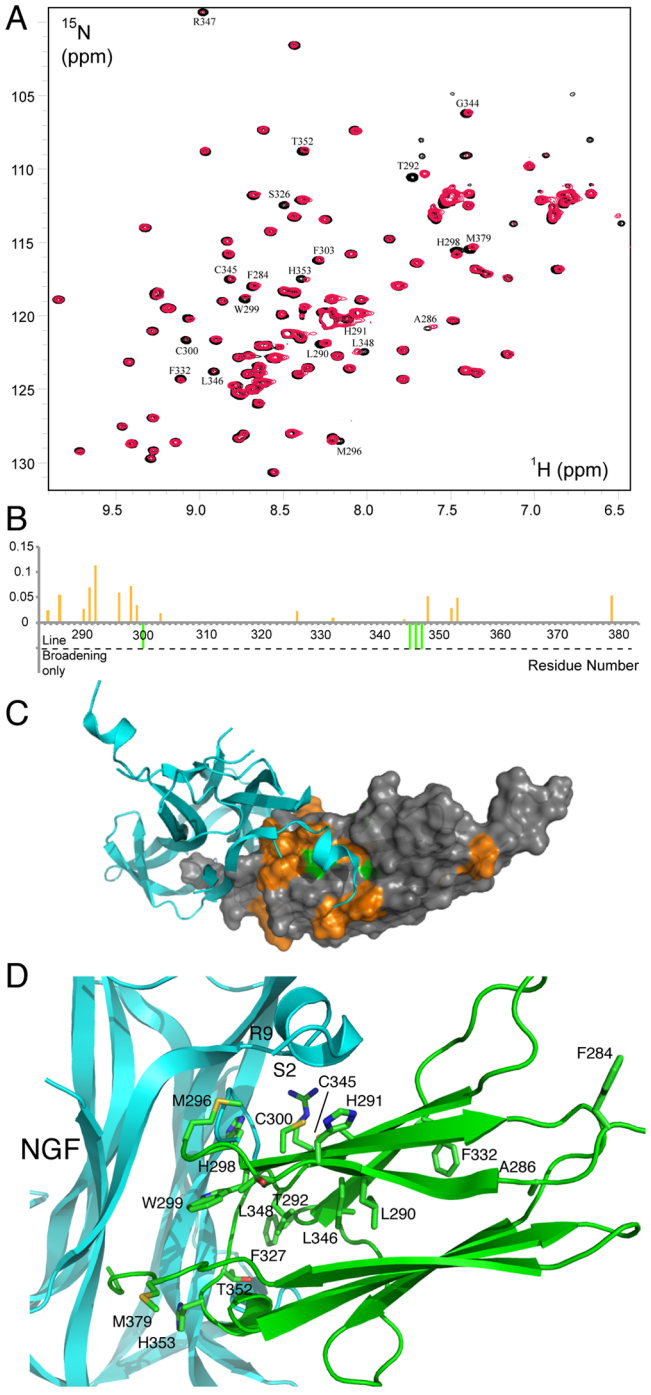

Figure 5. Interaction of NGF with TrkAIg2-NMR. (A) the overlaid ^{1}H−^{15}N HSQC spectra of TrkAIg2-NMR construct before (black) and after (red) the addition of stoichiometrically equivalent quantity of NGF. Resonances that show chemical shift perturbations (CSPs) or appear significantly broadened have been annotated. (B) $\Delta\delta_{NH}$ between free TrkAIg2-NMR and NGF present (orange), where the height is proportional to the difference in ppm. Negative green peaks indicate that line-broadening was observed but no CSP. The majority of the residues that show CSPs or line broadening interact with the N-terminus of NGF that forms a helix on binding the TrkAIg2 domain. (C) Surface representation of TrkAIg2-NMR (dark-gray) and NGF (cyan) with CSPs and line broadening shaded orange and exchange-broadened peaks only shaded green. (D) NGF (cyan) is depicted in secondary structure as a ribbon in complex with one TrkAIg2-NMR (green), with residues corresponding to the peaks shifted in the ^{1}H−^{15}N HSQC spectrum drawn as sticks.

the groove formed by strands β2, β4, and β5 that binds the N-terminal helix of NGF with several additional residues in the loop connecting strands β5 and β6.[5] In particular, residues which are almost completely line broadened (shown as green bars in Figure 5B) form a patch centered in the binding groove which would contact the helix (Figure 5C). This N-terminal helix is unstructured when NGF is crystallized in the free form (1BET.pdb), and electron density is only visible for this region when NGF is in complex with the TrkAIg2 domain (1WWW.pdb) and makes an energetically important contribution to the binding energy of the TrkAIg2/NGF interaction.[25] We note however that the observed peak broadening is not as pronounced as expected if a large, stable complex was formed with NGF (K_d low micromolar), suggesting that not all of the NGF was available in solution, perhaps due to binding to the glass of the NMR tube and the TrkAIg2-NMR remains well in excess.

The NGF and Amitriptyline Binding Sites Overlap. Next we tested whether we could observe an interaction of TrkAIg2-NMR with a small molecule ligand. The National Institute for Health and Clinical Excellence (NICE) supports the use of amitriptyline for the management of neuropathic pain, and therefore amitriptyline was one of a number of similar compounds tested in vitro by us and found to displace ^{125}I-NGF from human TrkA expressed on HEK cells (see below). Amitriptyline was therefore used in a NMR ^{1}H−^{15}N HSQC titration as a positive small molecule control. Addition of amitriptyline to TrkAIg2-NMR (100 μM) gave over 20 observable amide CSPs with five >0.2[24] (Figure 6B). The CSPs observed saturate with increasing amitriptyline concentration, allowing the extraction of the K_d values for four residues (T292 K_d 1.8 mM ± 0.2 mM, V305 K_d 2.1 mM ± 0.4 mM, C345 K_d 2.1 mM ± 0.4 mM, F303 K_d 2.2 mM ± 0.1 mM) (Figure 6C). The difference in K_d observed for amitriptyline binding to TrkAIg2-NMR versus the IC_{50} observed with full-length TrkA indicates some loss of affinity when utilizing this engineered single domain. Although the K_d is only in the mM range, this low molecular weight species (which lies within the <300 Da fragment classification) shows 13 common perturbed residues (CSP or line broadening) with NGF (Figures 5A and 6A,B) and include L290, T292, G344, C345, L346, and L348. These residues again map to the groove on the TrkAIg2 domain formed by strands β2, β4, and β5 and interconnecting loops where the N-terminal helix of NGF binds ("Site 1"). Several larger CSPs, however (e.g., S304 and V305), are only significantly perturbed by amitriptyline and arise from residues that lie within a narrower groove formed between stands β1 and β2 adjacent to the NGF helix binding site ("Site 2"). To further explore the bound conformation of amitriptyline, the compound was initially positioned by hand guided by the clustered CSPs at the known NGF binding site. Amitriptyline was then docked into the binding site on the TrkAIg2 domain using Bristol University Docking Engine (BUDE)[26] and poses judged against fits to the observed ^{1}H CSPs.[27] Seven of the top 10 poses from BUDE docking with best predicted binding energies were selected (see Supporting Information, Figure S4 and Table S1). A representative conformer from these models is shown in Figure 6D and covers both site 1 and site 2 defined by the CSPs. Amitriptyline binding in this position would be expected to interfere with NGF binding at site 1 as illustrated but does not completely occlude the NGF N-terminal helix binding groove (Figure 6D). The model also shows that amitriptyline binding extends somewhat beyond the binding site of the N-terminus of

dx.doi.org/10.1021/jm501307e | J. Med. Chem. 2015, 58, 767−777

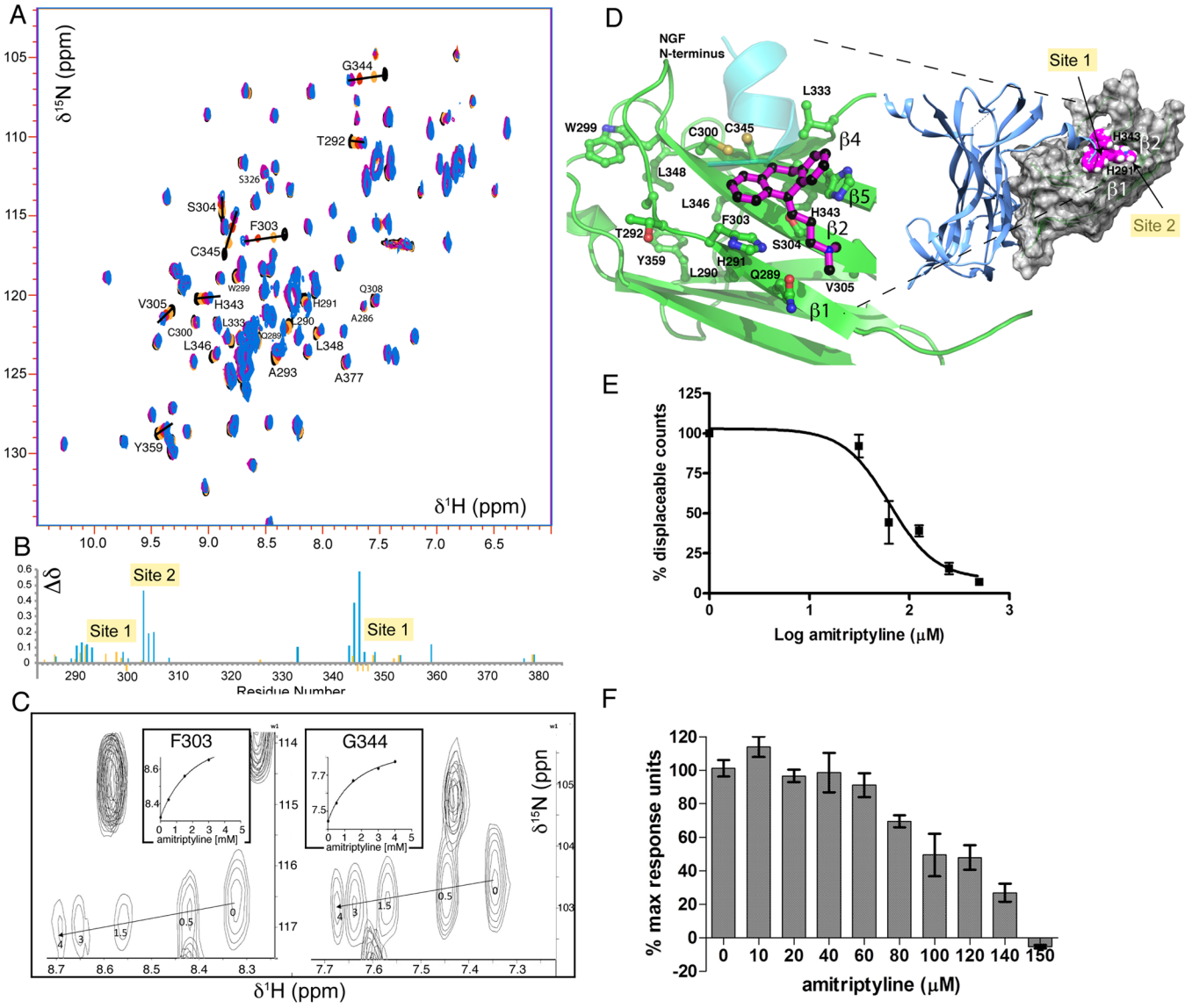

Figure 6. TrkAIg2-NMR constructs interacts with a small molecule, amitriptyline. (A) Peak shifts attributed to amitriptyline binding. (B) $\Delta\delta_{NH}$ between free and amitriptyline bound TrkAIg2-NMR (blue), where the height is proportional to the difference in ppm. Also shown are the CSPs for the interaction with NGF for comparison (orange). The negative points again indicate that line broadening was observed but no significant CSP. (C) Titration with amitriptyline provides a saturable signal. F303 and G344 show amide peaks shift with titrated amitriptyline, and both the change in peak positions and the resulting chemical shift change versus amitriptyline curves are shown as insets. (D) Amitriptyline docked into the groove identified by peak shifts and inset surface representation of amitriptyline docked into TrkAIg2-NMR. The N-terminal helix of NGF which is partially blocked (Site 1) by amitriptyline binding is shown in blue. Both H291 and H343 show CSPs. (E) Amitriptyline competes with radiolabeled NGF for binding to the full-length TrkA receptor expressed on HEK cells with $IC_{50} \sim 60\ \mu M$. (F) Amitriptyline antagonizes downstream signaling (phosphorylation of ERK 42/44) normally triggered by the NGF/TrkA interaction in automated immunofluorescence (InCell) assays (GE Healthcare) with an $EC_{50} \sim 86\ \mu M$.

NGF to site 2. This may have implications for the design of further small molecule binders targeting TrkA.

Amitriptyline Competes with NGF for Binding to the Full-Length Human TrkA Expressed on HEK Cells. Dose related displacement of ^{125}I-NGF by amitriptyline was assessed using a competition assay (see Materials and Methods). The acid salt of amitriptyline is freely soluble in water; therefore, to avoid any unforeseen effects, dimethyl sulfoxide (DMSO) was not used in any assays or NMR experiments. Our results showed that amitriptyline competes with radiolabeled NGF for binding to human TrkA with an IC_{50} 60 μM (Figure 6E). Automated immunofluorescence (InCell) analysis also shows that amitriptyline inhibits the phosphoERK signal induced downstream of TrkA activation by 0.5 nM NGF on HEK cells expressing the full-length human TrkA receptor with an EC_{50} of approximately 86 μM (Figure 6F). Evidence of competition with respect to NGF on cells expressing human TrkA corroborates the observed peak shifts on the TrkA-Ig2-NMR, both indicating binding site overlap between amitriptyline and NGF.

CONCLUSIONS

The TrkA/NGF interaction is an important and well-validated target for pain intervention. By modifying the TrkAIg2 domain, we have produced a valuable tool for assessing the binding of compounds to a site on TrkA in order to inhibit the binding of NGF. The main problems we have overcome were protein flexibility and strand-swapping at high concentrations. Protein flexibility was reduced by truncating the C-terminus to exclude

dx.doi.org/10.1021/jm501307e | J. Med. Chem. 2015, 58, 767−777

residues 384−413, and strand-swapping was abolished by the addition of a disulfide bond to "staple" together two intramolecular β-strands. The addition of five N-terminal aspartic acid residues further improved monomer yield in the refold. Overall, these mutations provided a stable construct, and the three-dimensional solution NMR structure has an identical fold to that of the TrkAIg2 domain in its native conformation bound to its cognate ligand NGF (pdb code 1WWW). The HSQC spectra are robustly reproducible between batches, facilitating the rapid determination of the weakly binding compound amitriptyline. Because of the construct being an excised domain, we observed a reduction in binding affinity versus the full-length receptor, however, this successfully located the binding site and generated CSP data of sufficient quality to be used as additional docking restraints by BUDE. Therefore, we suggest that in conjunction with traditional binding and functional assays TrkAIg2-NMR will be a useful tool in the hit to lead optimization of therapeutics as antagonists for pain or agonist/modulators for cholinergic support in Alzheimer's disease.

MATERIALS AND METHODS

Molecular Modeling. *Modeling the Disulfide Staple.* The residues chosen to form a disulfide staple were mutated using chain X from the crystal structure 1WWW.pdb in InsightII 2005. The complex was soaked with a 10 Å layer of water and then energy-minimized using Discover 2.98 (Accelrys Inc., San Diego, CA). During initial stages of minimization, all atoms were restrained. Subsequently, all atoms were gradually allowed freedom to move, enabling backbone and side chain flexibility as the system relaxed. Images were generated using a combination of Chimera (University of California San Francisco), Gimp (Gnu Image Manipulation Program, http://www.gimp.org/), and Powerpoint (Microsoft).

Docking Amitriptyline. Guided by the amide shifts induced by the binding of amitriptyline to the TrkAIg2-NMR construct, the compound was maneuvered into position by hand using InsightII. The complex was soaked with a 10 Å layer of water and then energy-minimized as described above. To verify this position, the docking software BUDE was used to dock amitriptyline into the center of the binding area highlighted by the peak shifts on HSQC. Fourteen different conformers of amitriptyline were produced and then allowed to rotate around 360° and translate by 12 Å in x, y, and z (a total of 8.25 million poses were sampled). Poses were initially ranked according to their BUDE predicted binding energy and subsequently by the minimum distance between any amitriptyline atom and the predominant amide, HN (proton) CSPs (T292, F303, S304, V305, H343, G344, C345, and L346) achieved by amitriptyline binding.[27]

Cloning of TrkAIg2-NMR. The TrkAIg2-NMR construct was produced in two stages. The TrkAIg2-DS1 construct represents residues 285−383 comprising the NGF binding domain of the human TrkA receptor (P04629). A full length TrkAIg2 domain 7.2cis pET24a (+) plasmid was used as a PCR template (residues 285−413). This template included P285C and P367C mutations and had been engineered to reduce mRNA secondary structure by the incorporation of silent mutations (residues 286−290) to favor ribosome binding. These silent mutations facilitated the eventual production of recombinant TrkAIg2-NMR within an *Escherichia coli* expression system.

Stage 1. Amplification of TrkAIg2-DS1 from TrkAIg2 d57.2cis pET24a(+) by PCR with Pfu polymerase (Promega) using primers (GGAATTCCATATGGATGACGATGACGATGTTAGCTTTTTGTGCTTCAGTACAATTA) and (CCGCTCGAGTTATCAGAAAGGGTTGTCCATGAAGGCAGCCATG) produced a PCR product that was subcloned into the NdeI and XhoI cloning sites of pET24a(+) vector (Novagen) and transformed into a nonexpression host XL1 blue (Stratagene). Purified mutant construct pET24a(+)TrkAIg2-DS1 was checked by sequencing and then transformed into a BL21(DE3) *E. coli* (Novagen) expression host.

Stage 2. The penta-Asp tagged TrkAIg2-NMR construct was made by amplification of the TrkAIg2-NMR from template pET24a(+)-TrkAIg2-DS1 by PCR with Pfu polymerase (Promega) using the following primers: Forward primer including an NdeI site (GGAATTCCATATGGATGACGATGACGATGTTAGCTTTTGTGCTTCAGTACAATTA) and the reverse primer incorporating an XhoI site (CCGCTCGAGTTATCAGAAAGGGTTGTCCATGAAGGCAGCCATG).

The amplified sequence corresponds to the DNA sequence:

ATGGATGACGATGACGATGTTAGCTTTTGTGCTTCAGTACAATTACACACGGCGGTGGAGATGCACCACTGGTGCATCCCCTTCTCTGTGGATGGGCAGCCGGCACCGTCTCTGCGCTGGCTCTTCAATGGCTCCGTGCTCAATGAGACCAGCTTCATCTTCACTGAGTTCCTGGAGCCGGCAGCCAATGAGACCGTGCGGCACGGGTGTCTGCGCCTCAACCAGCCCACCCACGTCAACAACGGCAACTACACGCTGCTGGCTGCCAACCCCTGCGGCCAGGCCTCCGCCTCCATCATGGCTGCCTTCATGGACAACCCTTTCTGATAA.

This corresponds to the protein sequence:

MDDDDDVSFCASVQLHTAVEMHHWCIPFSVDGQPAPSLRWLFNGSVLNETSFIFTEFLEPAANETVRHGCLRLNQPTHVNNGNYTLLAANPCGQASASIMAAFMDNPF.

Expression of ^{15}N or ^{13}C/^{15}N-Labeled TrkAIg2-NMR. To produce ^{15}N or ^{13}C, ^{15}N-labeled TrkAIg2-NMR, BL21(DE3)TrkAIg2-NMR, cells were grown overnight in 50 mL of M9 minimal media (42 mM Na_2HPO_4, 22 mM KH_2PO_4, 9 mM NaCl, 45 mM $CaCl_2$, 2 mM $MgSO_4$, 2 mg/mL thiamine (Sigma)), containing 0.2% D-glucose ^{13}C (for ^{13}C preparations only), (C6) (Cambridge Isotope Laboratories), 10 mM $^{15}NH_4Cl$, 99% (Cambridge Isotope Laboratories) and 0.5 mg/mL of kanamycin (Sigma) at 37 °C. The cells were then diluted 1:10 in fresh media and grown at 37 °C to an OD_{595} = 0.6. Isopropyl-D-thiogalactoside (IPTG; Sigma) was then added to 1 mM, and the cells were grown overnight. Unlabeled protein was produced using the same protocol as outlined here except that minimal media with nutrient additives were replaced by Luria−Bertani (LB) culture media throughout.

Cells (8 g wet weight) were harvested by centrifugation at 8000 rcf at 4 °C for 15 min and resuspended into 50 mL of ice-cold, sterile 10% (v/v) glycerol. Pellets were stored as 25 mL aliquots and frozen at −80 °C until required. Aliquots were processed to obtain a purified inclusion body pellet. Briefly, each bacterial pellet was disrupted using a French-Press and resuspended in 200 mL of ice-cold resuspension buffer (20 mM Tris pH 8.5, 10 mM EDTA) containing 100 mM NaCl and centrifuged at 9000 rcf at 4 °C for 60 min. Three further rounds of resuspension were then carried out with centrifugation at 9000 rcf at 4 °C for 30 min. Each pellet was resuspended in 100 mL of resuspension buffer with sequential additions of 1 M NaCl, 1% (v/v) Triton X-100, and 100 mM NaCl. Inclusion body pellets were stored overnight at −80 °C.

Refolding of ^{13}C/^{15}N-Labeled TrkAIg2-NMR. Each inclusion body pellet was resuspended in 50 mL of a solubilization buffer comprised of 8 M urea, 40 mM Tris pH 8.2, 100 mM NaCl, and 1 mM β-mercaptoethanol (BME) and rocked on a platform for 3 h at room temperature. Solubilized TrkAIg2-NMR was collected as supernatant by centrifugation at 9000 rcf for 1 h at 10 °C. Protein concentrations of soluble TrkAIg2-NMR were estimated by UV absorption of aromatic residues at 280 nm (molar extinction coefficient is 12740 M^{-1} cm^{-1}) and adjusted by dilution in solubilization buffer to 0.1 mg/mL (~8 μM). Diluted, soluble TrkAIg2-NMR was dialyzed 1:20 overnight against a dialysis buffer comprised of 20 mM Tris at pH 8.2, containing 50 mM NaCl, at 4 °C using 28 mm diameter dialysis tubing with a molecular weight cutoff (MWCO) of 3500 Da (Medicell International). The partially refolded TrkAIg2-NMR was again dialyzed 1:20 overnight against the dialysis buffer containing an additional 10 mM NaCl. Refolded TrkAIg2-NMR was centrifuged at 8000 rcf at 4 °C for 60 min to remove the majority of insoluble protein; the supernatant was collected and stored on ice.

Purification of ^{13}C/^{15}N-Labeled TrkAIg2-NMR. TrkAIg2-NMR supernatant was loaded onto a pre-equilibrated 5 mL HiTrap Q FF

column (Amersham Bioscience) at 5 mL/min on an AKTA fast protein liquid chromatogaph (FPLC) (Amersham Bioscience) protein purification system. The column was then re-equilibrated with 5 column volumes of buffer A (20 mM Tris pH 8.2, 10 mM NaCl). TrkAIg2-NMR was eluted over a linear gradient consisting of 20 column volumes starting with buffer A and ending with buffer B (20 mM Tris, pH 8.2, 1 M NaCl). The eluent was monitored at 280 nm. TrkAIg2-NMR eluted with a retention time 7.7 min; fractions were pooled and stored on ice. Prior to data acquisition, the pooled fractions of TrkAIg2-NMR were concentrated to 6.8 mg/mL within 16 mm diameter, 3500 Da MWCO dialysis tubing (Medicell International) using polyethylene glycol (PEG) 20 kDa (Sigma). The dialysis bag was then transferred to 2000× volume NMR buffer (100 mM sodium phosphate pH 6.9, 10 mM NaCl) and dialyzed overnight at 4 °C to exchange buffers and remove any low molecular weight contaminants in the PEG.

NMR and Structure Calculation. Initial $^{1}H-^{15}N$ HSQC experiments were acquired in NMR buffer, 20 °C (to compare TrkAIg2-NMR and TrkAIg2-WT at 100 μM concentration) on a Varian INOVA 600 MHz spectrometer equipped with a room temperature probe. Triple resonance experiment data were acquired at 20 °C with a cryoprobe equipped Varian VNMRS operating at 600 MHz to assign the backbone and side chain atoms. ^{15}N, ^{13}C NOESY-HSQC (nuclear Overhauser effect (enhancement) spectroscopy−heteronuclear single quantum correlation) experiments were acquired at 600 MHz for distance restraints. NMR data processing and analysis was performed with NMRPipe[28] and CcpNmr Analysis version 2.3.1.[29] TALOS-N and DANGLE were used to predict the backbone dihedral angles.[30,31] Structures were calculated iteratively with CNS 1.2 using ARIA2.3 protocol before being water refined using the RECOORD protocol.[32−34] Restraints for the introduced disulfide bond were added once the juxtaposition of the cysteine residues was observed in structure calculations. Final structures were checked with iCing (version r1156) (https://nmr.cmbi.ru.nl/icing/iCing.html) and PSVS (version 1.5) (http://psvs-1_5-dev.nesg.org/).[35] Figures and analyses were produced using PyMOL (The PyMOL Molecular Graphics System, version 1.5.0.4, Schrödinger, LLC). and the UCSF Chimera package (Chimera was developed by the Resource for Biocomputing, Visualization, and Informatics at the University of California, San Francisco (supported by NIGMS P41-GM103311)).[36] PROFIT v2.5.2 was used to calculate the RMSD between the closest to average NMR structure and chain X of 1WWW.pdb (Martin, A. C. R., http://www.bioinf.org.uk/software/profit/).

NMR Titrations. TrkAIg2-NMR was typically 100 μM in 100 mM sodium phosphate, 10 mM NaCl, pH 6.9. Data was collected on a Varian VNMRS 600 MHz NMR spectrometer equipped with a cryogenically cooled triple resonance probe head. For the amitriptyline (Sigma, purity >98% by TLC) titration, amitriptyline was added to the following final concentrations: 0, 0.015, 0.03, 0.06, 0.18, 0.3, 0.5, 1.5, 3, and 4 mM. For comparative NMR of the NGF/TrkAIg2 complex, a stoichiometric equivalent of NGF (preadjusted to pH 6.9) was added to the TrkAIg2-NMR and spectra collected. CSPs (ΔδNH) were calculated according to eq 1 given below by Pellecchia et al.[24]

$$\Delta\delta_{NH} = \left\{\frac{1}{2}[(\Delta\delta_H)^2 + 0.2(\Delta\delta_H)^2]\right\}^{1/2} \quad (1)$$

Analytical Ultracentrifugation (AUC). AUC sedimentation velocity experiments were conducted at 20 °C in a Beckman Optima XL-A analytical ultracentrifuge using an An-60 Ti rotor and sedimentation velocity cells equipped with a two-channel aluminum centerpiece and sapphire windows. Then 410 μL solutions at 80 μM protein concentration were loaded in the sample channel, and the reference channel was loaded with 420 μL of buffer. Samples were centrifuged at 55000 rcf (An-60 Ti rotor), with absorbance scans taken across a radial range of 5.8−7.3 cm at 3 min intervals to a total of 180 scans. Data were fitted to a continuous c(s) distribution model using SEDFIT at a 95% confidence level.[37] The baseline, meniscus, frictional coefficient (f/f_0), and systematic time-invariant and radial-invariant noise were fitted. The rmsd for the reported fit was 0.007 OD. The partial specific volume ($\bar{\nu}$) for the protein and the buffer densities and viscosities were calculated using SEDNTERP (http://sednterp.unh.edu/).

Native Gel Electrophoresis. The TrkAIg2-NMR construct has a theoretical p*I* of 4.52, therefore 12% polyacrylamide gel electrophoresis was carried under normal (basic) conditions with no added SDS and no BME in the loading buffer.

Gel Filtration. TrkAIg2-NMR and mouse NGF were applied to a gel filtration SuperdexTM 75 (10/300 GLS in XK16 column with 60 cm bed height) separately and as a 1:1 ratio complex (1 mg/mL of each). A calibration column was run in 50 mM phosphate buffer containing 150 μM NaCl at pH 7.4. A calibration curve with standard globular proteins ran according to protein molecular weight: Dextran blue (2000 kDa) (which runs at void volume), bovine serum albumin (BSA; 67 kDa), carbonic anhydrase (29 kDa), and cytochrome C (12.4 kDa); correlation of molecular weight with running volume (r^2 = 0.98)

Cell Line Maintenance. Cells expressing the full-length human TrkA receptors were grown as monolayers in DMEM containing 10% fetal calf serum (FCS) (v/v), 2 mM glutamine, 10 U/mL penicillin, 0.1 mg/mL streptomycin, and 0.5 mg/mL G418 in T75 tissue culture flasks. Parent HEK cells (lacking expressed Trk receptors) were grown in DMEM containing 10% FCS (v/v), 2 mM glutamine, and antibiotics but not G418. For assays, cells were detached from monolayers (90−95% confluent) using versene (phosphate buffered saline (PBS) with 1 mM EDTA pH 8) for 5 min at 37 °C and pelleted by centrifugation (165*g* for 5 min at room temperature).

Radioligand Competition Assays with Amitriptyline. Displacement of ^{125}I-labeled neurotrophin NGF by amitriptyline was assessed in HEK N3S cells expressing native human TrkA. The cell pellet was washed three times by repeated resuspension and centrifugation, using 10 mL of assay buffer (PBS pH 7.4) containing 0.5 mM $MgCl_2$ and 0.9 mM $CaCl_2$, 0.5 mg/mL bovine serum albumin, and 1 mg/mL glucose each time to remove any growth factors which may interfere with subsequent assays. Cells were passed through a 21-gauge needle to disrupt cell clumps. Following the final wash, the supernatant was removed; cells resuspended in 10 mL of assay buffer and counted using a hemocytometer. Cells were diluted to give a final cell number in the assay of 1×10^5 cells per tube. A positive control consisted of 100 nM unlabeled neurotrophin, negative control was assay buffer, added to the cells before 2 nM ^{125}I-labeled neurotrophin was pipetted into each tube. The cells were placed on a shaking platform for 30 min. Three 100 μL aliquots from each tube were spun through 5% sucrose in assay buffer to pellet the cells (20000*g* at 4 °C), frozen in solid CO_2−ethanol bath, and snipped (using adapted clippers to maintain reproducible depth of tip). ^{125}I-NGF in the cell pellet was counted with a gamma counter (LKB Wallac 1272). The assay was deemed to have been successful if the unlabeled NGF in the positive control was able to displace >90% of the counts compared with the negative control.

Automated Immunofluorescence (InCell) Assays (GE Healthcare) with Amitriptyline. HEK293 cells were resuspended in complete DMEM containing 10% FCS, 2 mM glutamine, 10 U/mL penicillin, 0.1 mg/mL streptomycin, and 0.5 mg/mL G418 as necessary. Cells were plated out at 1×10^4 in 100 μL per well into polylysine coated black-walled/clear bottomed 96-well plates (Corning CC692) and incubated at 37 °C overnight in 5% CO_2. Once cells had reached 70−80% confluence the serum concentration was reduced to 0.1% FCS overnight.

Half the plate was populated with parent cells and the other half with cells expressing full length glycosylated human TrkA. Parent and TrkA cells were exposed to the same controls and compounds to ensure the results expressed were receptor-specific and not due to, e.g., toxicity. Each plate had dose−responses in triplicate in the presence and absence of neurotrophin to detect antagonist and agonist activity under the same conditions. This was to ensure any responses were TrkA receptor-mediated.

Amitriptyline was added to the cells in PBS in 50 μL, with or without 0.5 nM NGF, respectively, for assessing antagonist or agonist activity and incubated for 5 min at 37 °C. Cells were washed once in ice-cold PBS (200 μL) and then placed on ice. Cells were fixed using 50 μL per well of 4% (w/v) paraformaldehyde in PBS and incubated for 30 min at room temperature. Cells were washed once with PBS (100 μL) and

dx.doi.org/10.1021/jm501307e | J. Med. Chem. 2015, 58, 767−777

permeabilized by adding 50 μL per well −20 °C methanol for 5 min followed by a further wash in PBS (100 μL). Nonspecific binding was reduced by incubating with 50 μL per well 10% goat serum in PBS at room temperature (2 h) and washed once with PBS (100 μL) before 30 μL per well at 1:500 dilution anti-phosphoERK (pERK) antibody (New England Biolabs Ltd.) was added to the wells. Plates were covered and incubated in a moist chamber overnight at 4 °C. The cells were washed three times in PBS prior to application of 30 μL per well of the secondary antibody goat anti-rabbit Alexa 546 (Invitrogen) at 1/300 in PBS plus 1% goat serum and 4′,6-diamidino-2-phenylindole (DAPI) (Sigma-Aldrich) 1 mg/mL diluted to 1/10000 for nuclear staining. Plates were incubated for 90 min in the dark at room temperature and then washed three times with 200 μL of PBS per well and stored in 200 μL of PBS at 4 °C until read in the InCell 1000 analyzer (GE Healthcare).

Data were collected using excitation λ 535 nm and emission λ 620 nm for 2000 ms exposure for AlexaFluor secondary antibody signal for ERK activation (pERK 1/2). DAPI (as nuclear stain) was assessed using λ excitation 360 nm and emission λ 460 nm with 600 ms exposure. Data were analyzed and presented as pERK intensity per cell.

NGF-Dependent Cell Proliferation in PC12 Cells. For effects of TrkAIg2-NMR on NGF-dependent PC12 cell proliferation or survival, CellTiter 96 aqueous nonradioactive cell proliferation reagents 3-(4,5-dimethylthiazol-2-yl)-5-(3-carboxymethoxyphenyl)-2-(4-sulfophenyl)-2*H*-tetrazolium, inner salt (MTS) and the electron coupling reagent phenazinemethosulfate (PMS) (Sigma) were added to cells as per manufacturer's instructions. Cells were seeded at a cell density of 10000 cells per well into 96-well plates containing 100 μL of complete cell culture media (DMEM, 1% (v:v) penicillin/streptomycin glutamine). Mouse NGF was added to give a final concentration of 5 ng/mL. Serial dilutions of TrkAIg2 or TrkAIg2-NMR were added to the wells. MTS and PMS solutions were then added with final concentrations of 333 μg/mL MTS and 25 μM PMS. The assay was performed in triplicate at incubation times of 1, 2, and 3 h at 37 °C with 5% CO_2 to allow color development. Absorbance at 490 nm was recorded on a BIOHIT BP-800 spectrophotometer (Helsinki, Finland).

Neurite Outgrowth Assay. ^{15}N labeled TrkAIg2-NMR construct was diluted to achieve a final concentration in the assay of 4.5 μM, 2.25 μM, 1.125 μM, 562 nM, 281 nM, and 140 nM. NGF (human recombinant, Sigma) evokes neurite outgrowth on PC12 cells at a concentration of 0.04 nM after 3 days incubation at 37 °C. Buffer controls with and without NGF were used to verify that any suppression of neurite outgrowth was due to the protein and not the buffer in which it was dissolved. A positive control consisted of TrkAIg2-WT. Other control wells consisting of PC12 cells with and without NGF (in media) were included to check for cell responsiveness. The cells were removed from 90% confluent T75 flask in versene and resuspended in complete media (Dulbecco's Modified Eagle Medium (DMEM) (Gibco BRL) supplemented with 10% (v/v) fetal bovine serum (FBS, Sigma), 1% (v/v) penicillin/streptomycin solution (Sigma), and 2 mM L-glutamine (Gibco BRL). The cell number was adjusted to 4×10^4 per mL and 0.5 mL cells were seeded into collagen coated 24-well plates, 0.5 mL per well. TrkAIg2-NMR construct protein was diluted to 2× final concentration in full media. Neurite outgrowth was assessed semi-quantitatively on a scale of 0−4 as described previously[38] The assay was valued in quadruplicate with wells blinded by two independent assessors.

■ ASSOCIATED CONTENT

Supporting Information

Biophysical characterization data for TrkAIg2 and TrkAIg2-NMR construct and in vitro assays for sequestration of NGF. This material is available free of charge via the Internet at http://pubs.acs.org.

Accession Codes

The ensembles of NMR structures and associated NMR chemical shifts have been deposited with the Protein Data Bank and BioMagResBank with accession codes 4CRP and 19824, respectively.

■ AUTHOR INFORMATION

Corresponding Authors

*Phone: +44 117 331 7163. E-mail: matt.crump@bristol.ac.uk.
*Phone: +44 117 41 4147901. E-mail: shelley.allen@bristol.ac.uk.

Author Contributions

⊥D.K.S. and C.W. are joint first authors; E-mail, deb.shoemark@bristol.ac.uk (D.K.S.), c.williams@bristol.ac.uk (C.W.).

Notes

The authors declare no competing financial interest.
#Deceased January 27, 2010.

■ ACKNOWLEDGMENTS

This work has been supported by Alzheimer's Research UK, Bristol Research into Alzheimer's and Care of the Elderly (BRACE), the MRC Severnside Alliance for Translational Research (SARTRE), the Alumni of the University of Bristol, The Sigmund Gestetner Trust Fund, and the Alzheimer's Society. We also thank the EPSRC Bristol Chemical Synthesis Doctoral Training Centre (EP/G036764/1) PhD studentship funding (A.J.B.). S.J.A. is a Sigmund Gestetner Senior Research Fellow.

■ ABBREVIATIONS USED

AD, Alzheimer's disease; AUC, analytical ultracentrifugation; BDNF, brain derived neurotrophic factor; BME, β-mercaptoethanol; CSPs, chemical shift perturbations; DAPI, 4′,6-diamidino-2-phenylindole; DMEM, Dulbecco's Modified Eagle Medium; DMSO, dimethyl sulfoxide; DRG, dorsal root ganglion; FCS, fetal calf serum; IB, inclusion body; Ig2, second immunoglobulin-like domain; IP3, inositol 1,4,5-trisphosphate; IPTG, isopropyl-D-thiogalactoside; TrkA, tyrosine kinase A; TrkAIg2, second immunoglobulin (and NGF binding) domain on TrkA; TrkAIg2-NMR, construct used for NMR; LB, Luria−Bertani; MAP kinase/ERK, mitogen-activated kinase/extracellular-signal-regulated kinase; MWCO, molecular weight cutoff; NGF, nerve growth factor; NMR, nuclear magnetic resonance; NOESY-HSQC, nuclear Overhauser effect spectroscopy−heteronuclear single quantum correlation; PEG, polyethylene glycol; PLC-γ, phospholipase C-γ; pERK, phosphorylated extracellular-signal-regulated kinase; PI3-kinase, phosphatidylinositol-3 kinase; rmsd, root-mean-square deviation; TRPV1, transient receptor potential cation channel vanilloid subfamily member 1

■ REFERENCES

(1) Allen, S. J.; Watson, J. J.; Shoemark, D. K.; Barua, N. U.; Patel, N. K. GDNF, NGF and BDNF as therapeutic options for neurodegeneration. *Pharmacol. Ther.* **2013**, *138*, 155−175.

(2) Watson, J. J.; Allen, S. J.; Dawbarn, D. Targeting nerve growth factor in pain. What is the therapeutic potential? *Biodrugs* **2008**, *22*, 349−359.

(3) Urfer, R.; Tsoulfas, P.; Oconnell, L.; Shelton, D. L.; Parada, L. F.; Presta, L. G. An immunoglobulin-like domain determines the specificity of neurotrophin receptors. *EMBO J.* **1995**, *14*, 2795−2805.

(4) Ultsch, M. H.; Wiesmann, C.; Simmons, L. C.; Henrich, J.; Yang, M.; Reilly, D.; Bass, S. H.; de Vos, A. M. Crystal structures of the neurotrophin-binding domain of TrkA, TrkB and TrkC. *J. Mol. Biol.* **1999**, *290*, 149−159.

(5) Wiesmann, C.; Ultsch, M. H.; Bass, S. H.; de Vos, A. M. Crystal structure of nerve growth factor in complex with the ligand-binding domain of the TrkA receptor. *Nature* **1999**, *401*, 184−188.

(6) Chuang, H. H.; Prescott, E. D.; Kong, H. Y.; Shields, S.; Jordt, S. E.; Basbaum, A. I.; Chao, M. V.; Julius, D. Bradykinin and nerve growth factor release the capsaicin receptor from PtdIns(4,5)P-2-mediated inhibition. *Nature* **2001**, *411*, 957−962.
(7) Zhuang, Z. Y.; Xu, H. X.; Clapham, D. E.; Ji, R. R. Phosphatidylinositol 3-kinase activates ERK in primary sensory neurons and mediates inflammatory heat hyperalgesia through TRPV1 sensitization. *J. Neurosci.* **2004**, *24*, 8300−8309.
(8) Priestley, J. V.; Michael, G. J.; Averill, S.; Liu, M.; Willmott, N. Regulation of nociceptive neurons by nerve growth factor and glial cell line derived neurotrophic factor. *Can. J. Physiol. Pharmacol.* **2002**, *80*, 495−505.
(9) Shu, X. Q.; Mendell, L. M. Nerve growth factor acutely sensitizes the response of adult rat sensory neurons to capsaicin. *Neurosci. Lett.* **1999**, *274*, 159−162.
(10) Watson, J. J.; Allen, S. J.; Dawbarn, D. Targeting nerve growth factor in pain: what is the therapeutic potential? *BioDrugs* **2008**, *22*, 349−59.
(11) Mok, S.-A.; Lund, K.; Campenot, R. B. A retrograde apoptotic signal originating in NGF-deprived distal axons of rat sympathetic neurons in compartmented cultures. *Cell Res.* **2009**, *19*, 546−560.
(12) Nassenstein, C.; Dawbarn, D.; Pollock, K.; Allen, S. J.; Erpenbeck, V. J.; Spies, E.; Krug, N.; Braun, A. Pulmonary distribution, regulation, and functional role of Trk receptors in a murine model of asthma. *J. Allergy Clin. Immunol.* **2006**, *118*, 597−605.
(13) Bishop, T.; Hewson, D. W.; Yip, P. K.; Fahey, M. S.; Dawbarn, D.; Young, A. R.; McMahon, S. B. Characterisation of ultraviolet-B-induced inflammation as a model of hyperalgesia in the rat. *Pain* **2007**, *131*, 70−82.
(14) Watson, J. J.; Fahey, M. S.; van den Worm, E.; Engels, F.; Nijkamp, F. P.; Stroemer, P.; McMahon, S.; Allen, S. J.; Dawbarn, D. TrkAd5: a novel therapeutic agent for treatment of inflammatory pain and asthma. *J. Pharmacol. Exp. Ther.* **2006**, *316*, 1122−1129.
(15) McNamee, K. E.; Burleigh, A.; Gompels, L. L.; Feldmann, M.; Allen, S. J.; Williams, R. O.; Dawbarn, D.; Vincent, T. L.; Inglis, J. J. Treatment of murine osteoarthritis with TrkAd5 reveals a pivotal role for nerve growth factor in non-inflammatory joint pain. *Pain* **2010**, *149*, 386−392.
(16) Hefti, F. F.; Rosenthal, A.; Walicke, P. A.; Wyatt, S.; Vergara, G.; Shelton, D. L.; Davies, A. M. Novel class of pain drugs based on antagonism of NGF. *Trends Pharmacol. Sci.* **2006**, *27*, 85−91.
(17) Brown, M. T.; Murphy, F. T.; Radin, D. M.; Davignon, I.; Smith, M. D.; West, C. R. Tanezumab reduces osteoarthritic knee pain: results of a randomized, double-blind, placebo-controlled phase III trial. *J. Pain* **2012**, *13*, 790−798.
(18) Halvorson, K. G.; Kubota, K.; Sevcik, M. A.; Lindsay, T. H.; Sotillo, J. E.; Ghilardi, J. R.; Rosol, T. J.; Boustany, L.; Shelton, D. L.; Mantyh, P. W. A blocking antibody to nerve growth factor attenuates skeletal pain induced by prostate tumor cells growing in bone. *Cancer Res.* **2005**, *65*, 9426−9435.
(19) Balanescu, A. R.; Feist, E.; Wolfram, G.; Davignon, I.; Smith, M. D.; Brown, M. T.; West, C. R. Efficacy and safety of tanezumab added on to diclofenac sustained release in patients with knee or hip osteoarthritis: a double-blind, placebo-controlled, parallel-group, multicentre phase III randomised clinical trial . *Ann. Rheum. Dis.* **2014**, *73*, 1665−1672 DOI: 10.1136/annrheumdis-2012-203164.
(20) Robertson, A. G. S.; Banfield, M. J.; Allen, S. J.; Dando, J. A.; Mason, G. G. F.; Tyler, S. J.; Bennett, G. S.; Brain, S. D.; Clarke, A. R.; Naylor, R. L.; Wilcock, G. K.; Brady, R. L.; Dawbarn, D. Identification and structure of the nerve growth factor binding site on TrkA. *Biochem. Biophys. Res. Commun.* **2001**, *282*, 131−141.
(21) Mason, J. M.; Gibbs, N.; Sessions, R. B.; Clarke, A. R. The influence of intramolecular bridges on the dynamics of a protein folding reaction. *Biochemistry* **2002**, *41*, 12093−12099.
(22) Cohen, S. Purification of a nerve-growth promoting protein from the mouse salivary gland and its neuro-cytotoxic antiserum. *Proc. Natl. Acad. Sci. U. S. A.* **1960**, *46*, 302−311.
(23) Pearce, F. L.; Banthorp, Dv; Cook, J. M.; Vernon, C. A. Adsorption of nerve growth-factor onto surfaces—implications for assay in tissue culture. *Eur. J. Biochem.* **1973**, *32*, 569−575.
(24) Pellecchia, M.; Sebbel, P.; Hermanns, U.; Wuthrich, K.; Glockshuber, R. Pilus chaperone FimC-adhesin FimH interactions mapped by TROSY-NMR. *Nature Struct. Biol.* **1999**, *6*, 336−9.
(25) Woo, S. B.; Timm, D. E.; Neet, K. E. Alteration of NH2-terminal residues of nerve growth factor affects activity and Trk binding without affecting stability or conformation. *J. Biol. Chem.* **1995**, *270*, 6278−6285.
(26) McIntosh-Smith, S.; Price, J.; Sessions, R. B.; Ibarra, A. A. High performance in silico virtual drug screening on many-core processors. *Int. J. High Perform. Comput. Appl.* **2014**, No. 1094342014528252.
(27) McCoy, M. A.; Wyss, D. F. Spatial localization of ligand binding sites from electron current density surfaces calculated from NMR chemical shift perturbations. *J. Am. Chem. Soc.* **2002**, *124*, 11758−11763.
(28) Delaglio, F.; Grzesiek, S.; Vuister, G. W.; Zhu, G.; Pfeifer, J.; Bax, A. NMRPipe: a multidimensional spectral processing system based on UNIX pipes. *J. Biomol. NMR* **1995**, *6*, 277−93.
(29) Vranken, W. F.; Boucher, W.; Stevens, T. J.; Fogh, R. H.; Pajon, A.; Llinas, M.; Ulrich, E. L.; Markley, J. L.; Ionides, J.; Laue, E. D. The CCPN data model for NMR spectroscopy: development of a software pipeline. *Proteins* **2005**, *59*, 687−96.
(30) Shen, Y.; Bax, A. Protein backbone and sidechain torsion angles predicted from NMR chemical shifts using artificial neural networks. *J. Biomol. NMR* **2013**, *56*, 227−241.
(31) Cheung, M.-S.; Maguire, M. L.; Stevens, T. J.; Broadhurst, R. W. DANGLE: A Bayesian inferential method for predicting protein backbone dihedral angles and secondary structure. *J. Magn. Reson.* **2010**, *202*, 223−233.
(32) Brunger, A. T. Version 1.2 of the Crystallography and NMR system. *Nature Protoc.* **2007**, *2*, 2728−2733.
(33) Nederveen, A. J.; Doreleijers, J. F.; Vranken, W.; Miller, Z.; Spronk, C. A. E. M.; Nabuurs, S. B.; Guntert, P.; Livny, M.; Markley, J. L.; Nilges, M.; Ulrich, E. L.; Kaptein, R.; Bonvin, A. M. J. J. RECOORD: A recalculated coordinate database of 500+ proteins from the PDB using restraints from the BioMagResBank. *Proteins: Struct., Funct., Bioinform.* **2005**, *59*, 662−672.
(34) Rieping, W.; Habeck, M.; Bardiaux, B.; Bernard, A.; Malliavin, T. E.; Nilges, M. ARIA2: Automated NOE assignment and data integration in NMR structure calculation. *Bioinformatics* **2007**, *23*, 381−382.
(35) Bhattacharya, A.; Tejero, R.; Montelione, G. T. Evaluating protein structures determined by structural genomics consortia. *Proteins* **2007**, *66*, 778−95.
(36) Pettersen, E. F.; Goddard, T. D.; Huang, C. C.; Couch, G. S.; Greenblatt, D. M.; Meng, E. C.; Ferrin, T. E. UCSF chimera—A visualization system for exploratory research and analysis. *J. Comput. Chem.* **2004**, *25*, 1605−1612.
(37) Brown, P. H.; Schuck, P. Macromolecular size-and-shape distributions by sedimentation velocity analytical ultracentrifugation. *Biophys. J.* **2006**, *90*, 4651−4661.
(38) Allen, S. J.; Robertson, A. G. S.; Tyler, S. J.; Wilcock, G. K.; Dawbarn, D. Recombinant human nerve growth factor for clinical trials: protein expression, purification, stability and characterisation of binding to infusion pumps. *J. Biochem. Biophys. Methods* **2001**, *47*, 239−255.